JOURNAL OF VIROLOGY, May 2008, p. 4656–4659 Vol. 82, No. 9
0022-538X/08/$08.00+0 doi:10.1128/JVI.02077-07

NOTES

Residue L143 of the Foot-and-Mouth Disease Virus Leader Proteinase Is a Determinant of Cleavage Specificity▽

Christina Mayer,[1]† David Neubauer,[1]† Aloysius T. Nchinda,[2] Regina Cencic,[1]‡ Katja Trompf,[1] and Tim Skern[1]*

Max F. Perutz Laboratories, Medical University of Vienna, Dr. Bohr-Gasse 9/3, A-1030 Vienna, Austria,[1] and Institute of Infectious Disease and Molecular Medicine, University of Cape Town, Observatory 7925, South Africa[2]

Received 19 September 2007/Accepted 7 February 2008

The foot-and-mouth disease virus (FMDV) leader proteinase (L^{pro}) self-processes inefficiently at the L^{pro}/VP4 cleavage site LysLeuLys*GlyAlaGly (* indicates cleaved peptide bond) when the leucine at position P2 is replaced by phenylalanine. Molecular modeling and energy minimization identified the L^{pro} residue L143 as being responsible for this discrimination. The variant L^{pro} L143A self-processed efficiently at the L^{pro}/VP4 cleavage site containing P2 phenylalanine, whereas the L143M variant did not. L^{pro} L143A self-processing at the eIF4GII sequence AspPheGly*ArgGlnThr was improved but showed more-extensive aberrant processing. Residue 143 in L^{pro} is occupied only by leucine and methionine in all sequenced FMDV serotypes, implying that these bulky side chains are one determinant of the restricted specificity of L^{pro}.

The foot-and-mouth disease virus (FMDV) is an animal pathogen of global concern (12). The FMDV leader proteinase (L^{pro}), an important determinant of pathogenicity, is a specific papain-like cysteine proteinase for which only two physiological roles have as yet been identified (8, 16). These are the self-processing reaction on the viral polyprotein in which L^{pro} frees itself from the growing polypeptide by cleaving between its own C terminus and the N terminus of VP4 (17) and a second reaction, the cleavage of the two homologues of the host protein eukaryotic initiation factor 4G (eIF4G), eIF4GI, and eIF4GII (6, 9, 11). These cleavages prevent cap-dependent translation and lead to the suppression or complete inhibition of host cell protein synthesis (6). Viral translation is unaffected since it initiates by an internal ribosome entry segment (1).

L^{pro} is the first protein encoded on the FMDV positive-sense RNA genome. Protein synthesis from this RNA can begin at one of two in-frame AUG codons separated by 28 amino acids (15). This leads to the production of two forms of L^{pro}, Lab^{pro} and Lb^{pro}; both forms have the same enzymatic activities (14). Lb^{pro} has been shown to be the form preferentially produced in vivo (3); therefore, all work presented here was performed with the shorter-version Lb^{pro} of FMDV $O1_k$.

The cleavage sites at which Lb^{pro} cleaves its substrates are LysLeuLys*GlyAlaGly (* indicates cleaved peptide bond) on the viral polyprotein and AsnLeuGly*ArgThrThr and AsnValGly*SerArgArg on eIF4GI and eIF4GII, respectively (9, 11). Surprisingly, the related sequence on eIF4GII, AspPheGly*ArgGlnThr, is not cleaved by Lb^{pro} (9). The variation among these cleavage sites has precluded a definition of a consensus sequence for Lb^{pro} and is in contrast with the extremely restricted specificity of this enzyme.

Kuehnel et al. (13) showed previously that in the self-processing reaction, Lb^{pro} does not efficiently recognize the eIF4GII sequence AspPheGly*ArgGlnThr. Analysis of Lb^{pro} cleavage on the sequence AspPheGly*ArgGlnThr showed that the presence of aspartic acid at the P3 position or phenylalanine at the P2 position impaired the Lb^{pro} self-processing reaction (13). The nomenclature of the cleavage sites and the corresponding binding sites on the enzyme is that of Berger and Schechter (2). The ability of cellular papain-like proteinases to accept or exclude aromatic amino acids at the P2 position depends heavily on the architecture of the generally hydrophobic S2 pocket (18). We therefore set out to determine which of the residues of the Lb^{pro} S2 pocket are responsible for the exclusion of phenylalanine.

We used the coordinates of the crystal structure of Lb^{pro} 1QOL (10) as a starting point to identify residues which could be substituted to enlarge the S2 pocket and enable it to accept phenylalanine. In this structure, the C terminus of one Lb^{pro} molecule is found in the active site of the adjacent one (Fig. 1A) and therefore gives an indication of how the P region of the viral polyprotein substrate is bound. The P2 leucine residue (L200) is accommodated in a hydrophobic cavity formed by the side chains of the residues P99, P100, A101, I141, L143, A149, and L178 and by the main-chain atoms of W52, F142, and H148. We used molecular modeling to replace the P2 leucine residue with the bulky aromatic phenylalanine and examine which residues in the S2 pocket might clash sterically with the modeled P2 residue. Molecular modeling experiments were performed using the Insight II software package (Accelrys,

* Corresponding author. Mailing address: Medical University of Vienna, Max F. Perutz Laboratories, Dr. Bohr-Gasse 9/3, 1030 Vienna, Austria. Phone: 43 1 4277 61620. Fax: 43 1 4277 9616. E-mail: timothy.skern@meduniwien.ac.at.

‡ Present address: Department of Biochemistry, McIntyre Medical Sciences Building, McGill University, Montreal, Quebec, Canada H3G 1Y6.

† These authors contributed equally to this work.

▽ Published ahead of print on 27 February 2008.

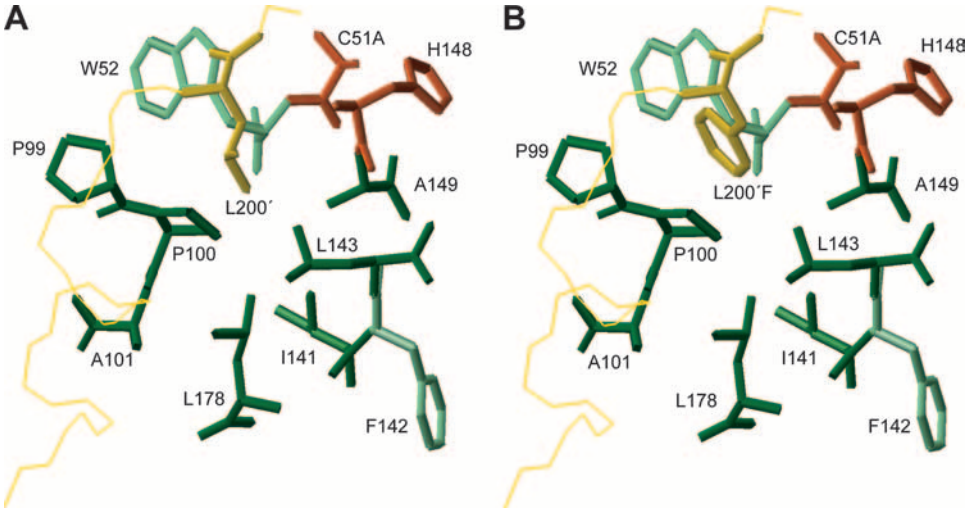

FIG. 1. The structure of the FMDV S2 pocket of Lb^{pro}. The side chains of the wild-type P2 residue L200 (A) and the modeled L200F mutation (B) after energy minimization are shown. Amino acid side chains comprising the pocket are dark green. Light-green residues contribute to the formation of the S2 pocket through main-chain interactions. Active-site residues are shown in red (C51 was replaced by alanine in the crystal structure (PDB code 1QOL) (10). The backbone of the C-terminal extension of the adjacent molecule is in yellow.

Inc., version 98.0) on a Silicon Graphics Octane I workstation. The structure of the phenylalanine at residue 200 (L200F) was generated with standard bond lengths and angles using the builder tools of Insight II software (Accelrys, Inc.). The root mean squared deviation value between the experimentally determined Lb^{pro} structure and the modeled Lb^{pro} structure was 1.53 Å.

Energy minimization of the modeled structure resulted in a 25.6-kcal/mol difference in total potential energy compared to the wild type. The consistent valence force field was used in all

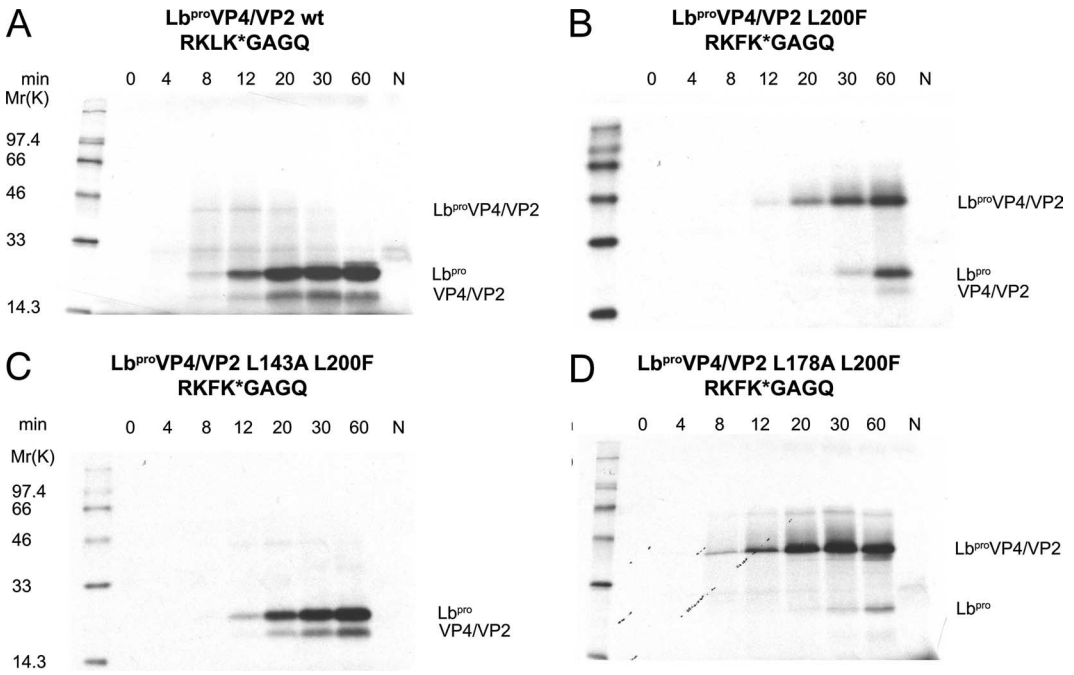

FIG. 2. Effect of mutations L143A and L178A on Lb^{pro} self-processing at the L/VP4 junction containing the substitution L200F. RRLs were incubated with or without 10 ng/μl of mRNAs encoding the wild type (Lb^{pro}VP4/VP2 wt) (A), Lb^{pro}VP4/VP2 L200F (B), Lb^{pro}VP4/VP2 L143A L200F (C), or Lb^{pro}VP4/VP2 L178A L200F (D). Ten-microliter samples were taken at the indicated time points, and protein translation was terminated by placing the samples on ice, followed by addition of unlabeled methionine and cysteine to final concentrations of 2 mM and Laemmli sample buffer. Ten-microliter aliquots were analyzed on a 17.5% sodium dodecyl sulfate-polyacrylamide gel, followed by fluorography. The negative controls (N) were incubated for 60 min without RNA. The amino acid sequences at the Lb^{pro}/VP4 junction are given. The positions of uncleaved Lb^{pro}VP4/VP2 and cleavage products Lb^{pro} and VP4/VP2 are marked. Protein standards (in kDa) are shown on the left.

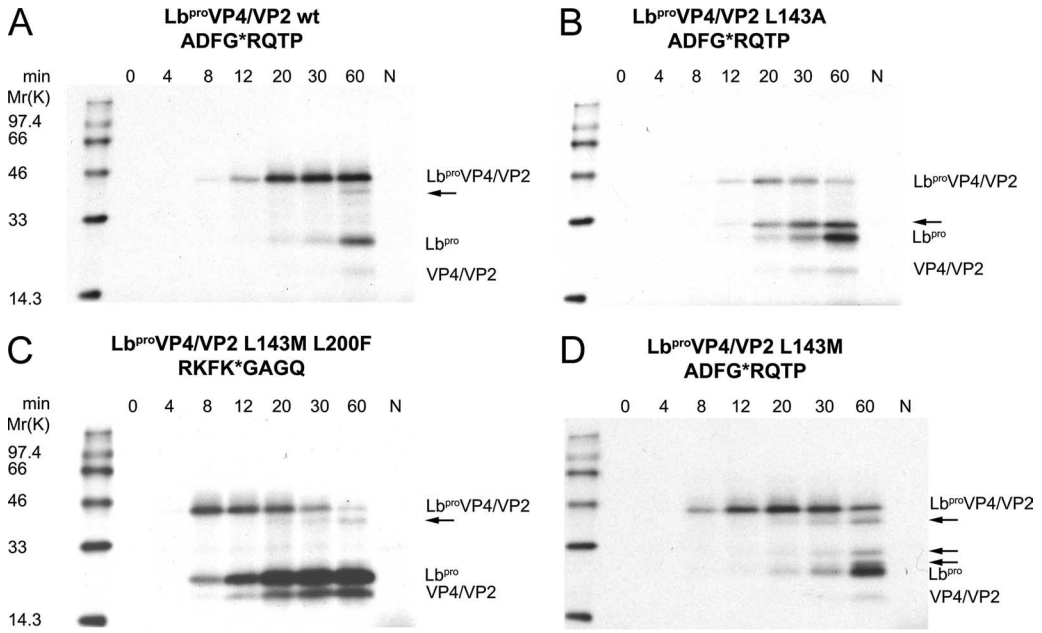

FIG. 3. Self-processing of the wild type (Lb^{pro}VP4/VP2 wt), Lb^{pro} L143A, and Lb^{pro} L143M on substrates containing phenylalanine at the P2 position. RRLs were incubated with the indicated mRNAs (10 ng/μl). In vitro protein synthesis and analysis were carried out as described in the legend to Fig. 2. The amino acid sequences at the Lb^{pro}/VP4 junction are shown above each panel. (A) Lb^{pro}VP4/VP2 wt on the eIF4GII sequence; (B) Lb^{pro}VP4/VP2 L143A on the eIF4GII sequence; (C) Lb^{pro}VP4/VP2 L143M on L200F; (D) Lb^{pro}VP4/VP2 L143M on the eIF4GII sequence. Protein standards (in kDa) are shown on the left. Aberrant cleavage products are marked with arrows.

energy minimizations and dynamic runs. The conjugate gradient minimization algorithm was also used after running the 1,000 initial steps, followed by 3,000 cycles of molecular dynamics and 3,000 cycles of energy minimizations in an NTV (native, i.e., constant number of atoms, temperature, and volume) ensemble at a temperature of 300 K. All calculations were carried out with a dielectric constant of 1.00 and with a cutoff distance of 9.50 Å. Figure 1B shows the minimized S2 pocket accommodating the P2 phenylalanine; the aromatic ring of phenylalanine comes closer to residues W52 and P100 than the aliphatic leucine side chain. Furthermore, the bulky side chain of L143 appears to prevent the aromatic phenylalanine P2 residue from penetrating deeper into the S2 pocket. This arrangement could explain the poor acceptance of phenylalanine at P2. We decided therefore to replace the long nonpolar side chain of L143 with the smaller side chain of alanine and investigate the ability of this variant to accept substrates containing phenylalanine at P2.

The self-processing activity of Lb^{pro} can be conveniently assayed with rabbit reticulocyte lysates (RRLs) (Fig. 2). An mRNA encoding the Lb^{pro} protein, all 85 amino acids of VP4, and 78 amino acids of VP2 was transcribed and used to direct protein synthesis in RRLs as reported previously (7). The translation products were separated by sodium dodecyl sulfate-polyacrylamide gel electrophoresis as described by Dasso and Jackson (5), and the newly synthesized [^{35}S]methionine-labeled proteins were detected by fluorography (7). Lb^{pro} is active upon synthesis, so that the mature products Lb^{pro} and VP4/VP2 are visible even after just 8 min (Fig. 2A). The effect of the substitution of leucine at P2 by phenylalanine (L200F) is shown in Fig. 2B. As reported by Kuehnel et al. (13), cleavage products were essentially not detected until 20 min after the start of translation. We then introduced the mutation L143A via site-directed mutagenesis into the plasmid Lb^{pro}VP4/VP2 L200F and examined Lb^{pro} processing in RRLs. Figure 2C shows that the presence of the L143A substitution was sufficient to completely restore the processing of the L200F variant to wild-type levels. As a control, we also investigated the effect of the mutation I141A, since the energy minimization had also indicated that this residue might be involved in influencing specificity at P2. In contrast to the result with L143, only a small improvement in cleavage of the L200F cleavage site was observed with the I141A substitution (data not shown). This emphasizes the importance of residue L143 in determining specificity.

Comparisons with other papain-like enzymes previously led us to propose that L178 might be important in excluding phenylalanine from the S2 site (13). However, our modeling and minimization experiments did not indicate that substituting L178 would improve the ability of the S2 pocket to accept phenylalanine. To examine the accuracy of the modeling prediction, we therefore examined the role of L178 by introducing the mutation L178A into the plasmid Lb^{pro}VP4/VP2 L200F and examined the efficiency of self-processing. Figure 2D shows that Lb^{pro} self-processing in this variant is even less efficient than with the original L200F mutation (compare Fig. 2D and B). This observation supports the predictions of the modeling. Thus, it appears that the overall architecture of the Lb^{pro} S2 pocket differs substantially from that of those cellular papain-like enzymes. This may result from the smaller number of residues found in the S2 pocket of FMDV Lb^{pro}.

We then investigated the ability of the Lb^{pro} L143A variant to perform self-processing at the sequence AspPheGly*ArgGlnThr present on eIF4GII. Figure 3A shows the inability of Lb^{pro} to perform self-processing of this sequence, as reported by Kuehnel et al. (13); the self-processing reaction commences

only about 60 min after the addition of RNA. Figure 3B shows that the Lb^{pro} L143A variant could indeed improve processing at this sequence. However, a significant amount of an aberrant product which was not present in the original variant was also observed (compare Fig. 3A and B). The inability of the Lb^{pro} L143A variant to process AspPheGly*ArgGlnThr to wild-type levels is presumably due to the presence of other nonoptimal residues in this cleavage sequence. For example, the presence of aspartate in place of lysine at the P3 position was shown to be detrimental to cleavage in the wild-type cleavage sequence. Thus, it will certainly be necessary to introduce further mutations in Lb^{pro} to achieve wild-type self-processing rates on the AspPheGly*ArgGlnThr sequence.

The above experiments emphasize the importance of L143 in restricting the specificity of Lb^{pro}. Examination of Lb^{pro} sequences from other FMDV serotypes reveals that residue 143 is not invariant (4). However, the only other residue occurring at this position is methionine, another residue with a bulky, hydrophobic side chain (4). This suggests that it is important for viral replication that Lb^{pro} does not process substrates containing phenylalanine at the P2 position. This notion is supported by the presence of only leucine or valine at the P2 position in the self-processing site in the polyproteins of FMDV (H. G. O'Neill, personal communication). To examine this idea further, we decided to investigate the ability of the Lb^{pro} 143M variant to carry out self-processing at L200F (Fig. 3C) and the eIF4GII sequence (Fig. 3D). Interestingly, the effect of the L200F mutation on self-processing by Lb^{pro} L143M was less detrimental than that seen on the wild type (compare Fig. 2B and 3C). In contrast, the effect on self-processing at the eIF4GII site was similar to that seen with wild-type Lb^{pro}, although more aberrant proteins were visible (compare Fig. 3A and D).

These results also imply that Lb^{pro} from most if not all serotypes will not cleave cellular proteins containing phenylalanine at the P2 position. Thus, the presence of leucine or methionine at residue 143 may restrict the number of possible substrates which can be cleaved during the FMDV replication cycle. Pertinently, the eIF4G homologues remain the only known cellular proteins which are cleaved by Lb^{pro} during the viral replication cycle. Furthermore, our recent intensive efforts using proteomics and bioinformatics techniques have failed to reveal any further proteins which are cleaved by Lb^{pro} during FMDV infection in cell culture.

In summary, these experiments show that the occupancy at residue 143 of Lb^{pro} determines to a significant extent the specificity of Lb^{pro} at the P2 position. The presence of leucine at residue 143 contributes substantially to the maintenance of the high degree of specificity of FMDV Lb^{pro}. Future work will investigate how the Lb^{pro} S3 pocket excludes aspartate while being able to accept asparagine and lysine.

This work was supported by the Austrian Science Foundation (grant P-17988 to T.S.).

We thank Ed Sturrock for critically reading the manuscript.

REFERENCES

1. **Belsham, G. J., and R. R. Jackson.** 2000. Translation initiation on picornavirus RNA, p. 869–900. *In* N. Sonenberg, J. W. B. Hershey, and M. B. Mathews (ed.), Translational control of gene expression, vol. 39. Cold Spring Harbor Press, Cold Spring Harbor, NY.
2. **Berger, A., and I. Schechter.** 1970. Mapping the active site of papain with the aid of peptide substrates and inhibitors. Philos. Trans. R. Soc. London B **257:**249–264.
3. **Cao, X., I. E. Bergmann, R. Fullkrug, and E. Beck.** 1995. Functional analysis of the two alternative translation initiation sites of foot-and-mouth disease virus. J. Virol. **69:**560–563.
4. **Carrillo, C., E. R. Tulman, G. Delhon, Z. Lu, A. Carreno, A. Vagnozzi, G. F. Kutish, and D. L. Rock.** 2005. Comparative genomics of foot-and-mouth disease virus. J. Virol. **79:**6487–6504.
5. **Dasso, M. C., and R. J. Jackson.** 1989. Efficient initiation of mammalian mRNA translation at a CUG codon. Nucleic Acids Res. **17:**6485–6497.
6. **Devaney, M. A., V. N. Vakharia, R. E. Lloyd, E. Ehrenfeld, and M. J. Grubman.** 1988. Leader protein of foot-and-mouth disease virus is required for cleavage of the p220 component of the cap-binding protein complex. J. Virol. **62:**4407–4409.
7. **Glaser, W., and T. Skern.** 2000. Extremely efficient cleavage of eIF4G by picornaviral proteinases L and 2A in vitro. FEBS Lett. **480:**151–155.
8. **Gorbalenya, A. E., E. V. Koonin, and M. M. Lai.** 1991. Putative papain-related thiol proteases of positive-strand RNA viruses. Identification of rubi- and aphthovirus proteases and delineation of a novel conserved domain associated with proteases of rubi-, alpha- and coronaviruses. FEBS Lett. **288:**201–205.
9. **Gradi, A., N. Foeger, R. Strong, Y. V. Svitkin, N. Sonenberg, T. Skern, and G. Belsham.** 2004. Cleavage of eukaryotic translation initiation factor 4GII within foot-and-mouth disease virus-infected cells: identification of the L-protease cleavage site in vitro. J. Virol. **78:**3271–3278.
10. **Guarné, A., J. Tormo, K. Kirchweger, D. Pfistermueller, I. Fita, and T. Skern.** 1998. Structure of the foot-and-mouth disease virus leader protease: a papain-like fold adapted for self-processing and eIF4G recognition. EMBO J. **17:**7469–7479.
11. **Kirchweger, R., E. Ziegler, B. J. Lamphear, D. Waters, H. D. Liebig, W. Sommergruber, F. Sobrino, C. Hohenadl, D. Blaas, R. E. Rhoads, and T. Skern.** 1994. Foot-and-mouth disease virus leader proteinase: purification of the Lb form and determination of its cleavage site on eIF-4 gamma. J. Virol. **68:**5677–5684.
12. **Kitching, R. P.** 2005. Global epidemiology and prospects for control of foot-and-mouth disease. Curr. Top. Microbiol. Immunol. **288:**133–148.
13. **Kuehnel, E., R. Cencic, N. Foeger, and T. Skern.** 2004. Foot-and-mouth disease virus leader proteinase: specificity at the P2 and P3 positions and comparison with other papain-like enzymes. Biochemistry **43:**11482–11490.
14. **Medina, M., E. Domingo, J. K. Brangwyn, and G. J. Belsham.** 1993. The 2 species of the foot-and-mouth disease virus leader protein, expressed individually, exhibit the same activities. Virology **194:**355–359.
15. **Sangar, D. V., S. E. Newton, D. J. Rowlands, and B. E. Clarke.** 1987. All foot and mouth disease virus serotypes initiate protein synthesis at two separate AUGs. Nucleic Acids Res. **15:**3305–3315.
16. **Skern, T., B. Hampoelz, A. Guarné, I. Fita, E. Bergmann, J. Petersen, and M. N. G. James.** 2002. Structure and function of picornavirus proteinases, p. 199–212. *In* B. L. Semler and E. Wimmer (ed.), Molecular biology of picornaviruses. ASM Press, Washington, DC.
17. **Strebel, K., and E. Beck.** 1986. A second protease of foot-and mouth disease virus. J. Virol. **58:**893–899.
18. **Turk, D., G. Guncar, M. Podobnik, and B. Turk.** 1998. Revised definition of substrate binding sites of papain-like cysteine proteases. Biol Chem. **379:** 137–147.